

1 **Assessment of Sea Ice Simulations in the CMIP5**

2 **Models**

3
4 **Qi Shu^{1,2}, Zhenya Song^{1,2}, Fangli Qiao^{1,2}**

5 1 {First Institute of Oceanography, State Oceanic Administration, Qingdao 266061}

6 2 {Key Lab of Marine Science and Numerical Modeling, SOA, Qingdao 266061}

7 Correspondence to: Fangli Qiao (qiaofl@fio.org.cn)

8 9 **Abstract**

10 The historical simulations of sea ice during 1979 to 2005 by the Coupled Model
11 Intercomparison Project Phase 5 (CMIP5) are compared with satellite observations,
12 Global Ice-Ocean Modeling and Assimilation System (GIOMAS) output data and
13 Pan-Arctic Ice Ocean Modeling and Assimilation System (PIOMAS) output data in
14 this study. Forty-nine models, almost all of the CMIP5 climate models and Earth
15 System Models with historical simulation, are used. For the Antarctic, multi-model
16 ensemble mean (MME) results can give good climatology of sea ice extent (SIE), but
17 the linear trend is incorrect. The linear trend of satellite-observed Antarctic SIE is
18 $1.29 \times 10^5 \text{ km}^2 \text{ decade}^{-1}$; only 1/7 CMIP5 models show increasing trends, and the
19 linear trend of CMIP5 MME is negative ($-3.36 \times 10^5 \text{ km}^2 \text{ decade}^{-1}$). For the Arctic,
20 both climatology and linear trend are better reproduced. Sea ice volume (SIV) is also
21 evaluated in this study, and this is a first attempt to evaluate the SIV in all CMIP5
22 models. Compared with the GIOMAS and PIOMAS data, the SIV values in both
23 Antarctic and Arctic are too small, especially for the Antarctic in spring and winter.
24 The GIOMAS Antarctic SIV in September is $19.1 \times 10^3 \text{ km}^3$, while the corresponding
25 Antarctic SIV of CMIP5 MME is $13.0 \times 10^3 \text{ km}^3$, almost 32% less. The Arctic SIV of
26 CMIP5 in April is $27.1 \times 10^3 \text{ km}^3$, which is also less than the PIOMAS SIV ($29.5 \times$

27 10^3 km^3). This means that the sea ice thickness simulated in CMIP5 is too thin
28 although the SIE is fairly well simulated.

29

30 **1. Introduction**

31 The Coupled Model Intercomparison Project Phase 5 (CMIP5) provides a very useful
32 platform for studying climate change. Simulations and projections by more than 60
33 state-of-the-art climate models and Earth System Models are archived under CMIP5.
34 Assessment of the performance of CMIP5 outputs is necessary for scientists to decide
35 which model outputs to use in their research and for model-developers to improve
36 their models. Here, we focus on the assessment of sea ice simulations under CMIP5
37 historical experiment. The CMIP5 data portal contains sea ice outputs from 49
38 coupled models. Many of these CMIP5 sea ice simulations have been evaluated and
39 several valuable studies have been published.

40 For the Antarctic, the main problem of the CMIP5 models is their inability to
41 reproduce the observed slight increase of sea ice extent (SIE). Turner et al. (2013) first
42 assessed CMIP5 Antarctic SIE simulations using 18 models, and summarized that the
43 majority of these models have too little SIE at the minimum sea ice period of
44 February, and the mean of these 18 models' SIE shows a decreasing trend over
45 1979-2005, opposite to the satellite observation that exhibits a slight increasing trend.
46 Polvani et al. (2013) used four CMIP5 models to study the cause of observed
47 Antarctic SIE increasing trend under the conditions of increasing greenhouse gases
48 and stratospheric ozone depletion. They concluded that it is difficult to attribute the
49 observed trend in total Antarctic sea ice to anthropogenic forcing. Zunz et al. (2013)
50 suggested that the model Antarctic sea ice internal variability is an important metric to
51 evaluate the observed positive SIE trend. Using simulations from 25 CMIP5 models,
52 Mahlstein et al. (2013) pointed that internal sea ice variability is large in the Antarctic
53 region and that both the observed and simulated trends may represent natural variation
54 along with external forcing.

55 For the Arctic, CMIP5 models offer much better simulations. Stroeve et al. (2012)
56 evaluated CMIP5 Arctic SIE trends using 20 CMIP5 models. They found that the
57 seasonal cycle of SIE was well represented, and that the simulated SIE decreasing
58 trend was more consistent with the observations over the satellite era than that of
59 CMIP3 models but still smaller than the observed. They also noted the spread in
60 projected SIE through the 21st century from CMIP5 models is similar to that from
61 CMIP3 models. Massonnet et al. (2012) examined 29 CMIP5 models, and provided
62 several important metrics to constrain the projections of summer Arctic sea ice
63 projection. Liu et al. (2013) also pointed out that CMIP5 projections have large
64 inter-model spread, but they also found that they could reproduce observed Arctic
65 ice-free time by reducing the large spread using two different approaches with 30
66 CMIP5 models.

67 These studies only used some of CMIP5 models' outputs because other CMIP5 model
68 outputs were not yet submitted. By now, all the CMIP5 participants have finished
69 their model runs and submitted their model outputs. So, here we will evaluate all
70 CMIP5 sea ice simulations, in an attempt to provide the community a useful
71 reference.

72 The rest of the paper is structured as follows. Section 2 presents sea ice data and
73 analysis methodology used in this study. Model assessment is given in section 3.
74 Conclusions and discussion are provided in section 4.

75

76 **2. Data and Methodology**

77 Sea ice simulations of CMIP5 historical runs from 49 CMIP5 coupled models are now
78 available. Monthly sea ice concentration (SIC) and sea ice thickness from these
79 models are used in this study. These outputs are published by the Earth System Grid
80 Federation (ESGF) (<http://pcmdi9.llnl.gov/esgf-web-fe/>) by each institute that is
81 responsible for its model. Although there are several ensemble realizations of each
82 CMIP5 model, the standard deviation between different ensemble realizations of each

83 model is small (Turner et al., 2013; Table 1). So, here we only choose the first
84 realization of each model for the analysis. CMIP5 historical runs cover the period
85 from 1850 to 2005, but the continuous sea ice satellite record only started in 1979; so
86 the period of 1979-2005 is chosen for the following analysis. Monthly
87 satellite-observed SIC is used in this study, which is based on the National
88 Aeronautics and Space Administration (NASA) team algorithm (Cavalieri et al., 1996)
89 provided by the National Snow and Ice Data Centre (NSIDC)
90 (<http://nsidc.org/data/seaice/>). Satellite observed sea ice extent used here is also from
91 NSIDC (<ftp://sidacs.colorado.edu/DATASETS/NOAA/G02135/>). Sea ice volume
92 (SIV) is an important index for assessment of sea ice simulation although direct
93 observations of SIV are very limited. SIV in the Antarctic used here is from the
94 Global Ice-Ocean Modeling and Assimilation System (GIOMAS)
95 (http://psc.apl.washington.edu/zhang/Global_seaice/index.html). SIV in the Arctic is
96 from Pan-Arctic Ice Ocean Modeling and Assimilation System (PIOMAS)
97 ([http://psc.apl.washington.edu/wordpress/research/projects/arctic-sea-ice-volume-ano-](http://psc.apl.washington.edu/wordpress/research/projects/arctic-sea-ice-volume-anomaly/)
98 [maly/](http://psc.apl.washington.edu/wordpress/research/projects/arctic-sea-ice-volume-anomaly/)). Note that SIV data from GIOMAS and PIOMAS are not observations but
99 model simulations with data assimilation. The climatology and linear trends of
100 CMIP5 simulated SIE, SIC and SIV are compared with satellite observations and
101 GIOMAS and PIOMAS data. CMIP5 simulated SIE is computed as the total area of
102 all grid cells where SIC exceeds 15%. SIV is computed as the sum of the product of
103 SIC, the area of grid cell and sea ice thickness of each grid cell. All gridded SIC and
104 sea ice thickness are re-gridded onto 1.0° longitude by 1.0° latitude grids before the
105 analysis is performed. In this study, spring is from March to May for the Arctic, and
106 from September to November for the Antarctic. Summer, autumn and winter are
107 defined accordingly.

108

109 **3. Results**

110 **3.1 Assessment of Antarctic sea ice simulations**

111 CMIP5 multi-model ensemble mean (MME) Antarctic climatological SIE compares
112 well with the satellite-observed SIE (Fig. 1a), but the inter-model spread is large.
113 Satellite observations show that the Antarctic SIE has the minimum value of 3.0
114 million square kilometers in February and the maximum value of 18.7 million square
115 kilometers in September. CMIP5 MME SIE has the minimum and maximum values
116 of 3.3 and 18.7 million square kilometers, respectively. The seasonal cycle of
117 observed SIE is well represented by the MME SIE of the 49 CMIP5 coupled models.
118 The simulated errors are very small for each month. The simulated SIE errors are
119 smaller than 15% of the observations, except for March and April SIE values, which
120 are a little less than 85% of the observations. One standard deviation of CMIP5
121 simulations, which is larger than 15% of the observations (Fig. 1a), show that CMIP5
122 coupled models have large spread each month in terms of Antarctic SIE. Large SIE
123 spread and small MME SIE errors indicate that we should use as many models as we
124 can when using CMIP5 outputs.

125 Figures 1b and 2 show that linear trends of CMIP5 MME Antarctic SIE do not agree
126 with the satellite observations. Many studies showed that Antarctic SIE has an
127 increasing trend since the end of 1970s (Cavalieri et al., 1997; Zwally et al., 2002;
128 Cavalieri et al., 2003; Turner et al., 2009). Satellite-observed Antarctic SIE has a
129 small increasing linear trend with the rate of $1.29 \times 10^5 \text{ km}^2 \text{ decade}^{-1}$ during
130 1979-2005, while CMIP5-simulated linear trend is $-3.36 \times 10^5 \text{ km}^2 \text{ decade}^{-1}$ (Fig. 1b).
131 Only eight out of 49 CMIP5 models have increasing linear trends as the observations.
132 This supports the conclusion by Polvani et al. (2013) that it is difficult to attribute the
133 observed Antarctic SIE trends to anthropogenic forcing. Figure 2 shows that the
134 monthly and seasonal trends of CMIP5-simulated Antarctic SIE also do not agree with
135 the observations. Observed Antarctic SIE shows increasing trends in each month and
136 each season, and the largest trend is in March and the autumn season. CMIP5 MME

137 SIE, however, has decreasing trends in each month and each season, and the largest
138 trend is in February and the summer season.

139 The trends of observed Antarctic SIC have large spatial differences (Fig. 3), but the
140 simulated Antarctic SIC trends are almost decreasing everywhere (Fig. 4). Figure 3
141 shows that decreasing SIC is mainly in the Antarctic Peninsula, which is one of the
142 three high-latitude areas showing rapid regional warming over the last 50 years
143 (Vaughan et al., 2003). SIC also decreases in the Bellingshausen Sea and the
144 Amundsen Sea in summer and autumn. The increasing SIC is mainly in the Ross Sea
145 all year round and in the Weddell Sea in summer and autumn. Figure 4 clearly shows
146 that CMIP5 MME SIC has decreasing trend everywhere except in the coast of the
147 Amundsen Sea and in part of the Ross Sea in spring and winter.

148 SIV depends on both sea ice coverage and sea ice thickness. SIV is more directly tied
149 to climate forcing than SIE. So, SIV is an important climate indicator in climate study.
150 Sea ice thickness data are mainly ship-based observations. For the Antarctic, the sea
151 ice thickness data based on ship-based observations are very limited. A climatological
152 $2.5^{\circ} \times 5.0^{\circ}$ gridded Antarctic sea ice thickness map was provided until 2008 (Worby et
153 al., 2008). Recently, there are several studies using satellite observations of sea ice
154 thickness (Kurtz and Markus, 2012; Xie et al., 2013). These observations provide
155 modelers with useful validation of their models. But, these data are not easily used to
156 long-term simulation validations by now because these data are not too long enough.
157 Here, we use GIOMAS data, which is from a global ice-ocean model (Zhang and
158 Rothrock, 2003) with data assimilation capability.

159 CMIP5 SIV simulations have more problems than the SIE simulations. The main
160 problems of CMIP5 Antarctic SIV simulations include too big SIV in summer, too
161 small SIV in winter, too large model spread, and wrong linear trend compared with
162 the GIOMAS data (Fig. 5). In February, Antarctic SIV from GIOMAS is 1.9×10^3
163 km^3 , while the CMIP5 MME is $2.7 \times 10^3 \text{ km}^3$. In September, GIOMAS SIV is $19.1 \times$
164 10^3 km^3 , while CMIP5 MME is only $13.0 \times 10^3 \text{ km}^3$, almost 32% less than the
165 GIOMAS. We can also see from Figure 5a that the model spread of Antarctic SIV in

166 CMIP5 is very large. The one standard deviation of modeled SIV is much larger than
167 15% of the GIOMAS data in every month. We checked the correlation between SIE
168 RMS error and SIV RMS error, and we can find that for the Antarctic the models with
169 small SIE RMS errors always have small SIV RMS errors. It means that for the
170 Antarctic models with a more realistic SIE mean state may result in a convergence of
171 estimates of SIV. Figure 5b shows that GIOMAS SIV has an increasing trend of 0.45
172 $\times 10^3 \text{ km}^3 \text{ decade}^{-1}$, while CMIP5 MME SIV has a decreasing trend of -0.36×10^3
173 $\text{ km}^3 \text{ decade}^{-1}$. If we check each CMIP5 model separately, we will also find only eight
174 out of the 49 CMIP5 models have increasing SIV trend that is consistent with the
175 GIOMAS.

176

177 **3.2 Assessment of Arctic sea ice simulations**

178 CMIP5 shows a quite good annual cycle of Arctic SIE, but the model error in winter
179 is larger than that in summer and model spread is large (Fig. 6a). Arctic SIE reaches
180 the maximum value of 15.7 million square kilometers in March, and reaches the
181 minimum value of 6.7 million square kilometers in September. The MME
182 climatological SIE compares well with the satellite-observed SIE. The modeled error
183 is less than 15% of the observations in every month. CMIP5 MME SIE is bigger than
184 the satellite observation in spring, and the modeled error is quite small at other times.
185 The model spread is large, with one standard deviation of CMIP5 models bigger than
186 15% of the observed SIE in every month (Fig. 6a). The model spread in winter is
187 larger than that in summer.

188 CMIP5 MME SIE shows a decreasing trend that is consistent with the satellite
189 observation, though the decreasing rate is a little smaller than that of the observation
190 (Figs. 6b and 7). The satellite-observed SIE linear trend over the period of 1979-2005
191 is $-4.35 \times 10^5 \text{ km}^2 \text{ decade}^{-1}$, while CMIP5 MME SIE linear trend is only -3.71×10^5
192 $\text{ km}^2 \text{ decade}^{-1}$. Thirty-one out of the 49 CMIP5 models have smaller decreasing rate
193 than the observation. Both observed and CMIP5-simulated SIE in autumn has the

194 largest decreasing trend. CMIP5-simulated difference of SIE decreasing trend
195 between summer and autumn is, however, larger than that of the observations. The
196 main reason is CMIP5-simulated SIE has small reduction in summer, especially in
197 July (Fig. 7). Satellite-observed SIE decreasing rate is 5.22% per decade in July, while
198 the CMIP5-simulated decreasing rate is 3.54% per decade. The largest decreasing rate
199 is in September; the observed trend is -8.61% per decade and the simulated trend is
200 -8.46% per decade.

201 Figure 8 and 9 show that the spatial patterns of CMIP5-simulated SIC reduction rate
202 are consistent with the observations from 1979 to 2005, but the decreasing rates are
203 smaller than the observed. In spring and winter, the observed decreasing SIC is
204 mainly in the Okhotsk Sea, Baffin Bay, Greenland Sea and Barents Sea;
205 CMIP5-simulated decreasing SIC is also in these regions. In summer and autumn, the
206 main decreasing SIC is in the Chukchi Sea, Barents Sea and Kara Sea (Figs. 8 and 9),
207 and CMIP5 MME SIC has similar characteristics. However, CMIP5 simulations have
208 larger trends in the central Arctic Ocean.

209 The main problem of CMIP5 simulations is too little Arctic SIV all year round and
210 too large model spread (Fig. 10). In spring, the Arctic has the largest SIV. Long-term
211 mean PIOMAS SIV is maximum in April with $29.5 \times 10^3 \text{ km}^3$, but the corresponding
212 CMIP5 MME is only $27.1 \times 10^3 \text{ km}^3$. Long-term mean PIOMAS SIV is minimum in
213 April with $13.3 \times 10^3 \text{ km}^3$, but the corresponding CMIP5 MME is only $9.6 \times 10^3 \text{ km}^3$.
214 CMIP5 SIV model spread is also very large: one standard deviation for each month is
215 much larger than 15% of PIOMAS SIV. Arctic SIV declined significantly during
216 1979-2005, at a rate of $-2.14 \times 10^3 \text{ km}^3 \text{ decade}^{-1}$; CMIP5 MME trend has the same
217 sign but smaller, at $-1.45 \times 10^3 \text{ km}^3 \text{ decade}^{-1}$.

218

219 **4. Conclusions and discussion**

220 The first ensemble member of the 49 CMIP5 historical simulations was evaluated, in
221 terms of the performance of sea ice (Tables 1 and 2). The Arctic sea ice simulations

222 are better than the Antarctic sea ice simulations, and SIE simulations are better than
223 SIV simulations. CMIP5 MME SIV is too less in winter and spring because the sea
224 ice thickness in CMIP5 models is too thin in winter and spring compared with the
225 GIOMAS and PIOMAS data. For the Antarctic sea ice, the model internal variability
226 is an important metric to evaluate the observed positive SIE trend (Zunz et al., 2013).
227 For the Arctic sea ice, model mean state and seasonal cycle are important to Arctic sea
228 ice projection (Massonnet et al., 2012), so model mean state, cycle amplitude and
229 variability are also included in Tables 1 and 2. In the Antarctic, MME can reproduce
230 good mean state and monthly amplitude for SIE, but for SIV MME mean state and
231 amplitude are smaller. In the Arctic, MME can reproduce good mean state and
232 monthly amplitude for both SIE and SIV. CMIP5 simulations have very different
233 variability (indicated by standard deviation of detrended monthly SIE and SIV) for
234 different models. From Tables 1 and 2 we can conclude that the performance of each
235 model is different. For the Antarctic, ACCESS1.0, BCC-CSM1.1,
236 CESM1-CAM5-1-FV2, CMCC-CM, EC-EARTH, GISS-E2-H-CC, MIROC-ESM,
237 MIROC-ESM-CHEM, MRI-CGCM3, MRI-ESM1 and NorESM1-M can give better
238 SIE and SIV mean state. For the Arctic, ACCESS1.3, CCSM4, CESM1-BGC,
239 CESM1-CAM5, CESM1-CAM5-1-FV2, CESM1-FASTCHEM, EC-EARTH,
240 MIROC5, NorESM1-M and NorESM1-ME can give better mean state of SIE and SIV.
241 The Arctic SIE linear trends of BNU-ESM, CanCM4, CESM1-FASTCHEM,
242 EC-EARTH, GFDL-CM2p1, HadCM3, HadGEM2-AO, MIROC-ESM-CHEM,
243 MPI-ESM-MR and MRI-ESM1 are closed to the observations.

244 Both satellite-observed Antarctic SIE and GIOMAS Antarctic SIV show increasing
245 trends over the period of 1979-2005, but CMIP5 MME Antarctic SIE and SIV have
246 decreasing trends. Only eight models' SIE and another eight models' SIV show
247 increasing trends. Can these few CMIP5 models give correct Antarctic sea ice trend?
248 If we use these eight CMIP5 models to plot Antarctic SIC trends (not shown) as in Fig.
249 4, we will find that these eight CMIP5 model mean SIC trends have different spatial
250 patterns with the observations (Fig. 3) although their model mean SIE and SIV have

251 increasing trends. Satellite observed Antarctic SIE has increased trends, but when we
252 use satellite observed sea ice record, we should also keep in mind that satellite
253 observed sea ice record may also has large uncertainty. Eisenman et al. (2014) point
254 out that sensor transition may cause a substantial change in the long-term trend.

255 We can see that the CMIP5 MME does a good job in terms of climatological mean,
256 but their inter-model spread is large. The number of models used in published studies
257 is usually less than the total CMIP5 models. How many models can give similar good
258 simulations as all the available CMIP5 models? We first choose the CMIP5 models
259 randomly. The model number changes from 1 to 49. We then calculate the SIE and
260 SIV root mean square (RMS) errors between MME and observations or GIOMAS and
261 PIOMAS datasets. For each fixed model number, we choose these models randomly
262 many times, and then calculate the mean of the RMS errors. Figure 11 shows the ratio
263 of SIE and SIV RMS errors between the errors calculated using different number of
264 CMIP5 models and the errors calculated using all 49 CMIP5 models. We can see that
265 the model errors decrease quickly as the model number increases; and the more
266 models we use, the smaller error we have. For a fixed model number, the ratios of SIE
267 are larger than the ratios of SIV, and Antarctic SIE has the largest ratio. When the
268 model number is greater than 30, the model errors do not change much anymore. If
269 we choose a criterion of RMS error larger than 15% of all the model RMS error, the
270 model number of 22 is the critical number for Arctic SIE. It means that more than 22
271 CMIP5 models should give similar MME as all 49 CMIP5 models.

272

273 **Acknowledgments**

274 Satellite-observed sea ice concentration data are provided
275 by <http://nsidc.org/data/seaice/>, sea ice extent are from
276 <ftp://sidads.colorado.edu/DATASETS/NOAA/G02135/>, GIOMAS sea ice data are
277 downloaded from http://psc.apl.washington.edu/zhang/Global_seaice/index.html, and
278 PIOMAS sea ice data are from
279 <http://psc.apl.washington.edu/wordpress/research/projects/arctic-sea-ice-volume-ano>

280 maly/. CMIP5 sea ice simulations are downloaded
281 from <http://pcmdi9.llnl.gov/esgf-web-fe/>. The authors thank the above data providers.
282 This work is supported by the National Basic Research Program of China (973
283 Program) under Grant 2010CB950500, National Natural Science
284 Foundation of China(Grant no. 41306206), and the Project of Comprehensive
285 Evaluation of Polar Areas on Global and Regional Climate Changes
286 (CHINARE2014-04-04, CHINARE2014-04-01, and CHINARE2014-01-01).

287 **References**

288 Cavalieri, D. J., Parkinson, C. L., Gloersen, P., and Zwally, H.: Sea Ice Concentrations
289 from Nimbus-7 SMMR and DMSP SSM/I-SSMIS Passive Microwave Data, Boulder,
290 Colorado USA: NASA DAAC at the National Snow and Ice Data Center, 1996.

291 Cavalieri, D. J., Gloersen, P., Parkinson, C. L., Comiso, J. C., and Zwally, H. J.:
292 Observed hemispheric asymmetry in global sea ice changes, *Science*, 278(5340),
293 1104-1106, 1997.

294 Cavalieri, D. J., Parkinson, C. L., and Vinnikov, K. Y: 30-Year satellite record reveals
295 contrasting Arctic and Antarctic decadal sea ice variability, *Geophysical Research*
296 *Letters*, 30, 1970, doi:10.1029/2003GL018031, 2003.

297 Eisenman, I., Meier, W. N., and Norris, J. R.: A spurious jump in the satellite record:
298 has Antarctic sea ice expansion been overestimated?, *The Cryosphere*, 8, 1289-1296,
299 doi:10.5194/tc-8-1289-2014, 2014.

300 Kurtz, N., and Markus T.: Satellite observations of Antarctic sea ice thickness and
301 volume, *Journal of Geophysical Research*, 117, doi:10.1029/2012JC008141, 2012.

302 Liu, J., Song, M., Horton, R. M., and Hu, Y.: Reducing spread in climate model
303 projections of a September ice-free Arctic, *Proceedings of the National Academy of*
304 *Sciences*, 110(31), 12571-12576 , 2013.

305 Mahlstein, I., Gent, P. R., and Solomon, S.: Historical Antarctic mean sea ice area, sea
306 ice trends, and winds in CMIP5 simulations, *Journal of Geophysical Research:*
307 *Atmospheres*, 118(11), 5105-5110, 2013.

308 Massonnet, F., Fichefet, T., Goosse, H., Bitz, C. M., Philippon-Berthier, G., Holland,
309 M. M., and Barriat, P.-Y.: Constraining projections of summer Arctic sea ice, *The*
310 *Cryosphere*, 6, 1383-1394, doi:10.5194/tc-6-1383-2012, 2012.

311 Polvani, L. M., and Smith, K. L.: Can natural variability explain observed Antarctic
312 sea ice trends? New modeling evidence from CMIP5, *Geophysical Research Letters*,
313 40(12), 3195-3199, 2013.

314 Stroeve, J. C., Kattsov, V., Barrett, A., Serreze, M., Pavlova, T., Holland, M., and
315 Meier, W. N.: Trends in Arctic sea ice extent from CMIP5, CMIP3 and observations,
316 *Geophysical Research Letters*, 39, L16502, doi:10.1029/2012GL052676, 2012.

317 Turner, J., Comiso, C., Marshall, G. J., Lachlan-Cope, T. A., Bracegirdle, T., Maksym,
318 T., Meredith, M. P., Wang, Z., and Orr, A.: Non-annular atmospheric circulation
319 change induced by stratospheric ozone depletion and its role in the recent increase of
320 Antarctic sea ice extent, *Geophysical Research Letters*, 36, L08502,
321 doi:10.1029/2009GL037524, 2009.

322 Turner, J., Bracegirdle, T. J., Phillips, T., Marshall, G. J., and Hosking, J. S.: An Initial
323 Assessment of Antarctic Sea Ice Extent in the CMIP5 Models, *Journal of Climate*, 26,
324 1473–1484, doi: <http://dx.doi.org/10.1175/JCLI-D-12-00068.1>, 2013.

325 Vaughan, D. G., Marshall, G. J., Connolley, W. M., Parkinson, C., Mulvaney, R.,
326 Hodgson, D. A., King, J. C., Pudsey, C. J., and Turner, J.: Recent rapid regional
327 climate warming on the Antarctic Peninsula, *Climatic Change*, 60(3), 243-274, 2003.

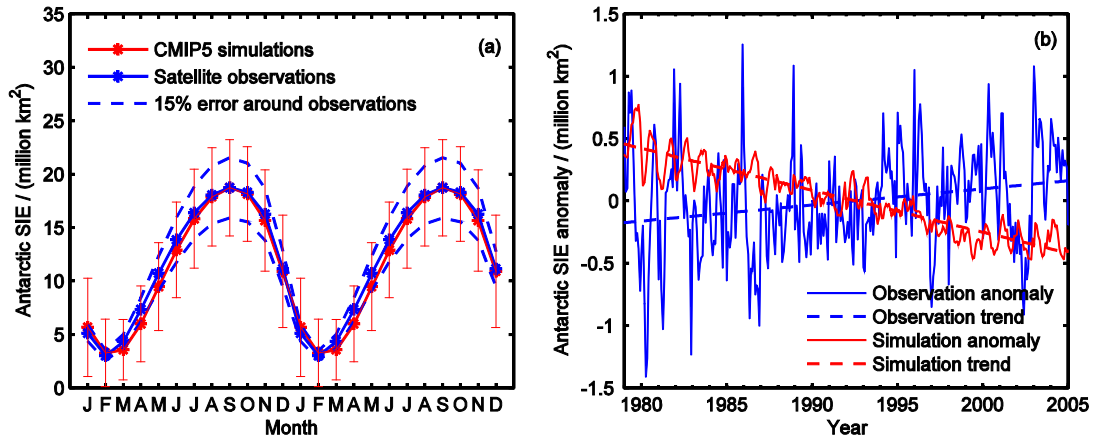
328 Worby, A. P., Geiger, C. A., Paget, M. J., Van Woert, M. L., Ackley, S. F., and
329 DeLiberty, T. L.: Thickness distribution of Antarctic sea ice, *Journal of Geophysical*
330 *Research: Oceans*, 113, C05S92, doi:10.1029/2007JC004254, 2008.

331 Xie, H., Tekeli, A. E., Ackley, S. F., Yi, D., and Zwally, H. J.: Sea ice thickness
332 estimations from ICESat altimetry over the Bellingshausen and Amundsen Seas,
333 2003–2009, *Journal of Geophysical Research: Oceans*, 118(5), 2438-2453, 2013.

334 Zhang, J., and Rothrock, D.: Modeling global sea ice with a thickness and enthalpy
335 distribution model in generalized curvilinear coordinates, *Monthly Weather Review*,
336 131, 845–861, 2003.

337 Zunz, V., Goosse, H., and Massonnet, F.: How does internal variability influence the
338 ability of CMIP5 models to reproduce the recent trend in Southern Ocean sea ice
339 extent?, *The Cryosphere*, 7, 451-468, doi:10.5194/tc-7-451-2013, 2013.

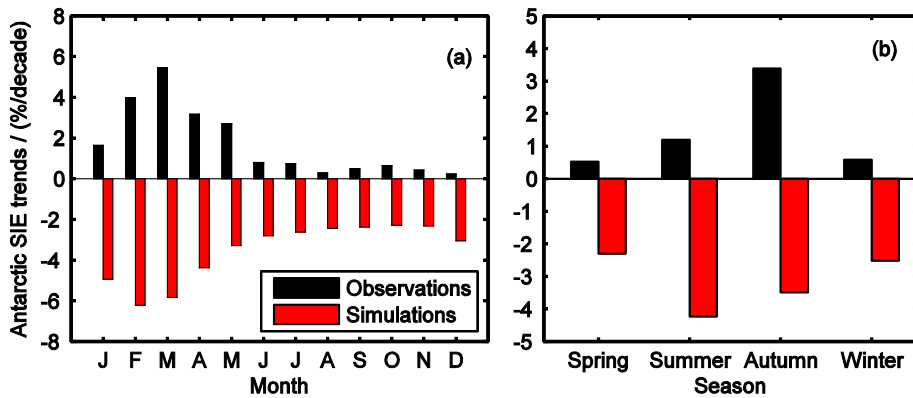
340 Zwally, H. J., Comiso, J. C., Parkinson, C. L., Cavalieri, D. J., and Gloersen, P.:
341 Variability of Antarctic sea ice 1979–1998, *Journal of Geophysical Research: Oceans*,
342 107(C5), 9-1-9-19, 2002.



343

344 Figure 1. Climatology (a), anomaly and linear trend (b) of satellite observed and
 345 CMIP5 simulated Antarctic sea ice extent during 1979-2005. Two annual cycles are
 346 plotted in (a). The error bar is the range of one standard deviation.

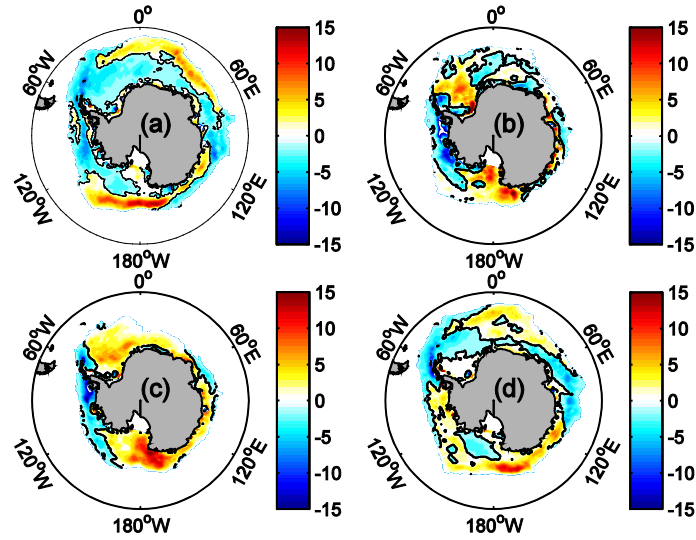
347



348

349 Figure 2. Monthly (a) and seasonal (b) linear trends of satellite observed and
 350 CMIP5-simulated Antarctic sea ice extent during 1979-2005.

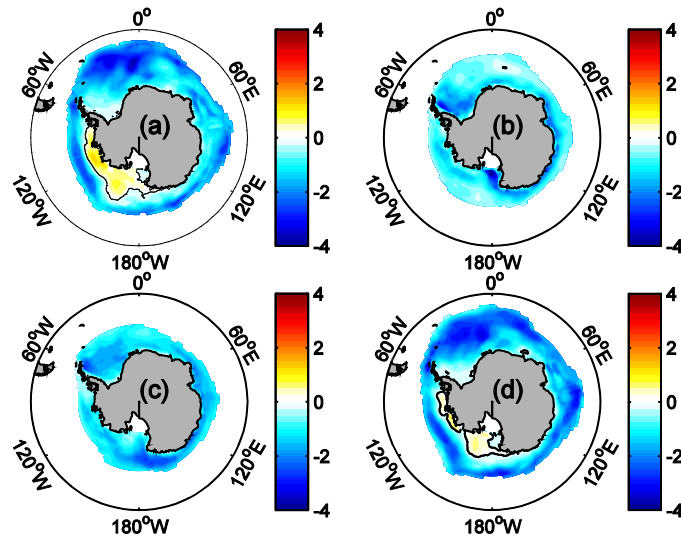
351



352

353 Figure 3. Linear trends (unit: % per decade) of satellite observed Antarctic sea ice
 354 concentration during 1979 to 2005. (a) Spring, (b) summer, (c) autumn, and (d)
 355 winter.

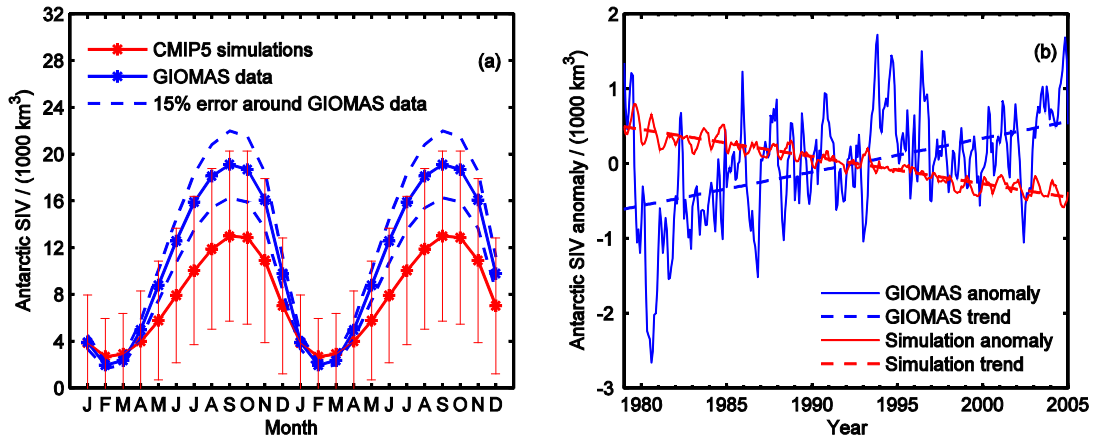
356



357

358 Figure 4. Linear trends (units: % per decade) of CMIP5-simulated Antarctic sea ice
 359 concentration during 1979-2005. (a) Spring, (b) summer, (c) autumn, and (d) winter.

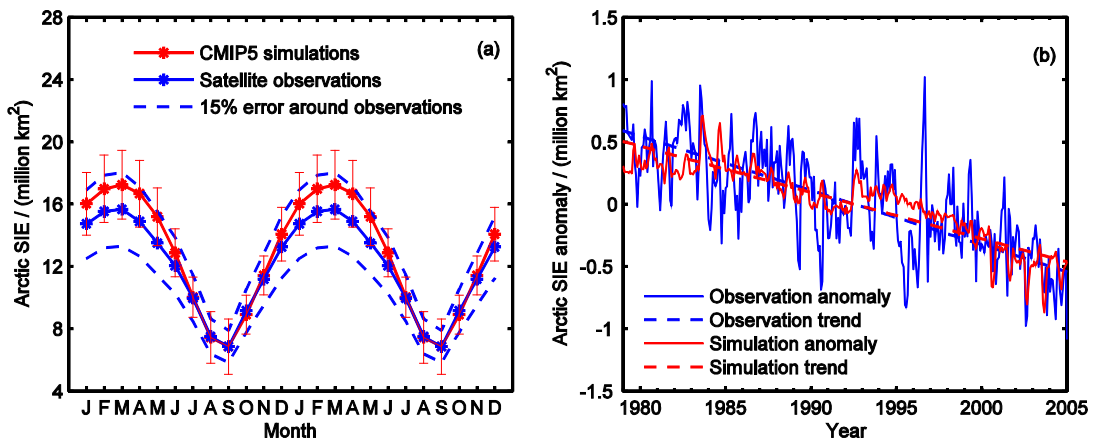
360



361

362 Figure 5. Climatology (a), anomaly and linear trend (b) of GIOMAS and CMIP5
 363 simulated Antarctic sea ice volume during 1979-2005. Two annual cycles are plotted
 364 in (a). The error bar is the range of one standard deviation.

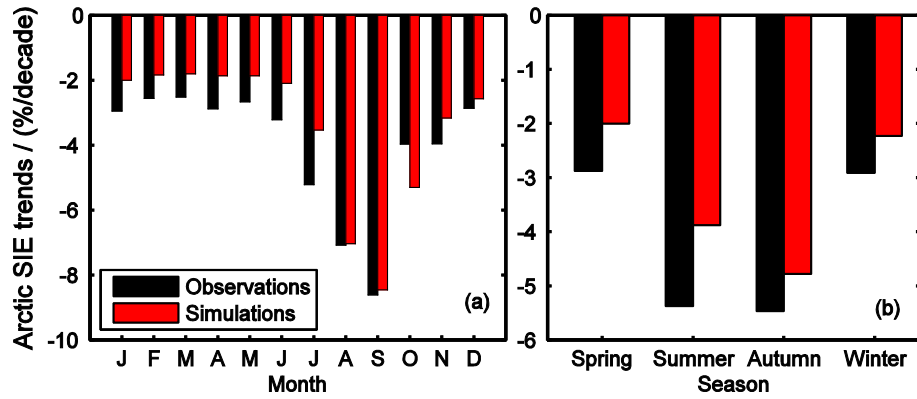
365



366

367 Figure 6. Climatology (a), anomaly and linear trend (b) of satellite observed and
 368 CMIP5-simulated Arctic sea ice extent during 1979-2005. Two annual cycles are
 369 plotted in (a). The error bar is the range of one standard deviation.

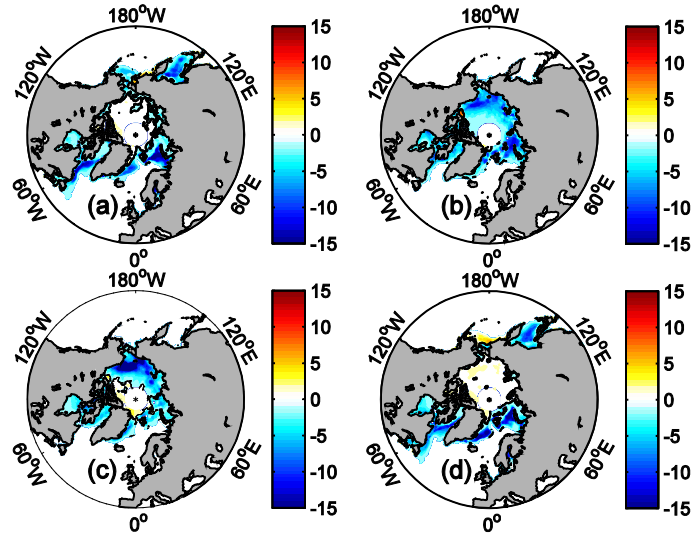
370



371

372 Figure 7. Monthly (a) and seasonal (b) linear trends of satellite observed and
 373 CMIP5-simulated Arctic sea ice extent during 1979-2005.

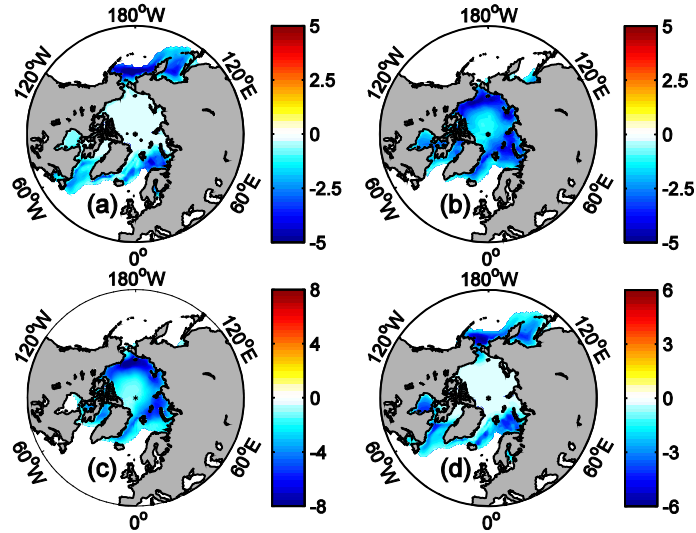
374



375

376 Figure 8. Linear trends (units: % per decade) of satellite observed Arctic sea ice
 377 concentration during 1979-2005. (a) Spring, (b) summer, (c) autumn, and (d) winter.

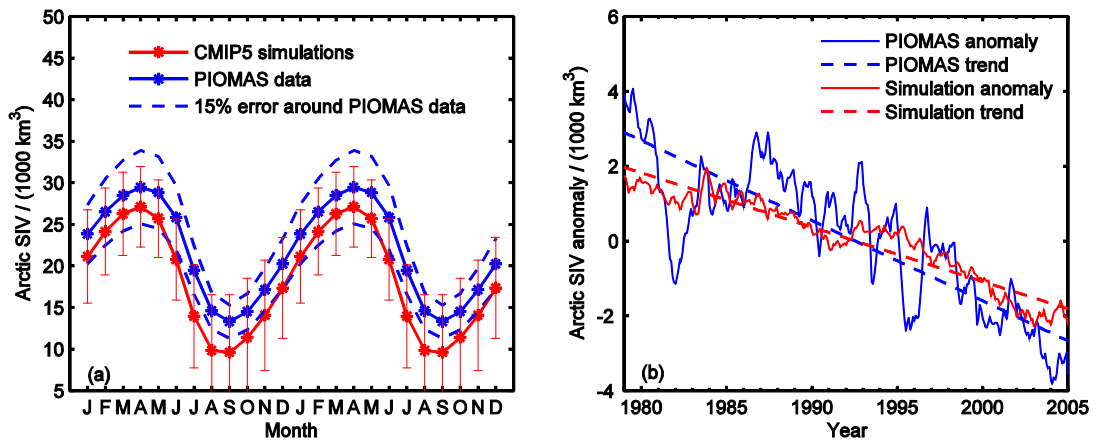
378



379

380 Figure 9. Linear trends (units: % per decade) of CMIP5-simulated Arctic sea ice
 381 concentration during 1979-2005. (a) Spring, (b) summer, (c) autumn, and (d) winter.

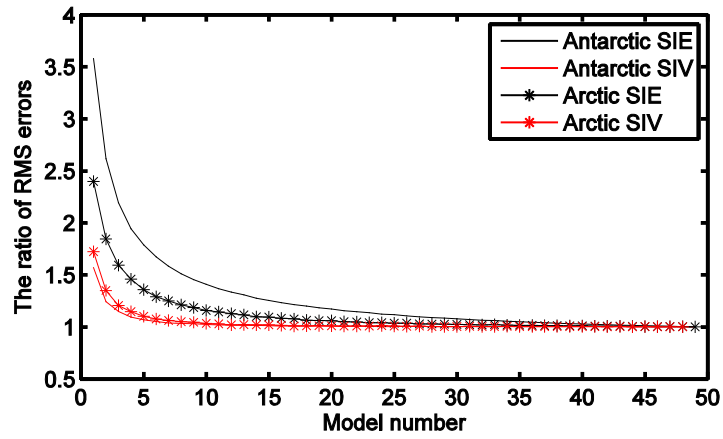
382



383

384 Figure 10. Climatology (a), anomaly and linear trend (b) of PIOMAS and
 385 CMIP5-simulated Arctic sea ice volume during 1979-2005. Two annual cycles are
 386 plotted in (a). The error bar is the range of one standard deviation.

387



388

389 Figure 11. The ratio of SIE and SIV RMS errors between the errors calculated using
390 different number of CMIP5 models and the error calculated using all 49 CMIP5
391 models.

392

393 Table 1. Antarctic sea ice metrics in CMIP5 models, satellite observations and GIOMAS dataset. Column (a) is mean annual SIE in million km².
394 Column (b) is monthly SIE amplitude in million km². Column (c) is standard deviation of detrended monthly SIE anomaly in million km².
395 Column (d) is linear trend in monthly SIE in 10⁵ km² decade⁻¹. Column (e) is monthly SIE room mean square error in million km². Column (f) is
396 mean annual SIV in 10³ km³. Column (g) is monthly SIV amplitude in 10³ km³. Column (h) is standard deviation of detrended monthly SIV
397 anomaly in 10³ km³. Column (i) is linear trend in monthly SIV in 10³ km³ decade⁻¹. Column (j) is monthly SIV room mean square error in 10³
398 km³.

Data sources or CMIP5 models	(a)	(b)	(c)	(d)	(e)	(f)	(g)	(h)	(i)	(j)
Observations or GIOMAS	11.94	15.70	0.40	1.29	----	11.02	17.17	0.63	0.45	----
Multi-model ensemble mean (MME)	11.50	15.46	0.11	-3.36	0.71	7.73	10.31	0.10	-0.36	4.20
ACCESS1.0	12.10	19.12	0.59	-1.72	1.57	6.30	11.35	0.43	-0.15	5.20
ACCESS1.3	14.24	15.77	0.54	-0.97	2.31	10.71	9.78	0.67	-0.03	2.75
BCC-CSM1.1	13.42	19.32	1.27	2.71	2.11	7.13	11.51	0.92	0.09	4.41
BCC-CSM1-1-M	12.26	18.86	1.06	-20.03	1.52	5.65	9.98	0.71	-1.20	5.92
BNU-ESM	20.60	23.46	0.82	-9.60	9.19	18.49	22.48	0.87	-2.03	7.89
CanCM4	14.65	20.58	0.74	-2.79	3.40	3.09	4.81	0.28	-0.06	9.21
CanESM2	14.69	20.64	0.96	-7.74	3.42	3.09	4.82	0.40	-0.15	9.22
CCSM4	18.37	13.70	0.58	-7.34	6.64	19.34	18.63	1.12	-1.56	8.34

Data sources or CMIP5 models	(a)	(b)	(c)	(d)	(e)	(f)	(g)	(h)	(i)	(j)
CESM1-BGC	17.67	14.05	0.49	-6.68	5.93	18.28	18.31	0.91	-1.19	7.28
CESM1-CAM5	14.06	14.78	0.47	-5.52	2.58	11.22	16.05	0.58	-0.97	1.13
CESM1-CAM5-1-FV2	13.01	14.11	0.58	-3.16	1.77	9.96	14.12	0.74	-0.22	1.89
CESM1-FASTCHEM	17.86	13.42	0.60	-8.78	6.14	18.41	18.15	1.18	-1.70	7.42
CESM1-WACCM	14.33	12.57	0.39	-6.45	2.95	11.55	13.15	0.66	-0.91	1.80
CMCC-CESM	11.84	19.43	0.99	2.91	2.01	6.70	11.18	0.71	0.26	4.91
CMCC-CM	11.81	16.84	0.67	-2.49	0.90	6.82	10.14	0.48	-0.05	4.97
CMCC-CMS	11.74	19.33	0.87	-1.52	1.83	6.31	10.70	0.59	-0.12	5.34
CNRM-CM5	7.78	16.98	0.77	-2.59	4.53	3.01	7.81	0.42	-0.10	8.79
CNRM-CM5-2	9.28	14.08	1.08	4.29	3.16	4.93	9.78	1.02	0.38	6.77
CSIRO-Mk3.6	15.92	12.11	0.67	-1.64	4.89	12.13	13.28	0.65	-0.29	2.62
EC-EARTH	10.66	17.18	0.66	-7.94	1.72	6.09	9.44	0.58	-0.66	5.75
FGOALS-g2	17.10	17.29	0.48	-1.47	5.28	15.65	13.89	0.74	-0.14	4.88
FIO-ESM	17.19	12.21	0.49	-8.53	5.61	21.23	13.98	1.16	-1.57	10.31
GFDL-CM2p1	8.00	15.38	0.81	-6.33	4.01	2.45	5.55	0.30	-0.19	9.57
GFDL-CM3	6.25	12.06	0.73	-6.82	5.82	1.92	4.16	0.37	-0.30	10.29
GFDL-ESM2G	8.11	14.34	0.63	-4.45	3.90	2.71	5.81	0.41	-0.24	9.31
GFDL-ESM2M	6.39	12.23	0.41	-1.61	5.65	1.81	4.20	0.16	-0.09	10.36
GISS-E2-H	6.21	10.62	0.38	-1.89	6.03	3.24	7.19	0.27	-0.24	8.65

Data sources or CMIP5 models	(a)	(b)	(c)	(d)	(e)	(f)	(g)	(h)	(i)	(j)
GISS-E2-H-CC	12.18	19.07	0.75	-5.75	1.52	6.70	14.16	0.51	-0.54	4.57
GISS-E2-R	7.74	14.31	1.01	-3.39	4.31	3.06	6.17	0.47	-0.16	8.92
GISS-E2-R-CC	8.12	14.55	0.66	0.82	3.93	3.12	6.24	0.35	0.00	8.86
HadCM3	14.26	19.95	0.78	-2.74	3.28	14.70	21.87	0.83	-0.49	4.13
HadGEM2-AO	9.11	14.29	0.59	-5.31	3.20	5.58	9.70	0.49	-0.42	6.26
HadGEM2-CC	9.12	14.29	0.72	-0.85	3.25	5.50	9.68	0.61	-0.05	6.34
HadGEM2-ES	9.82	15.02	0.70	-3.25	2.60	6.16	10.33	0.61	-0.41	5.66
INMCM4	6.25	10.91	0.48	-4.00	6.04	2.81	6.12	0.38	-0.28	9.21
IPSL-CM5A-LR	9.66	19.06	0.84	-5.03	3.43	4.13	8.66	0.53	-0.26	7.70
IPSL-CM5A-MR	8.08	17.30	0.74	1.69	4.56	2.80	6.50	0.35	0.01	9.21
IPSL-CM5B-LR	3.34	8.09	0.42	0.59	9.09	1.22	3.32	0.20	0.04	11.10
MIROC4h	10.90	17.53	0.61	-7.96	1.33	5.35	9.74	0.41	-0.51	6.28
MIROC5	3.23	6.62	0.29	-1.03	9.29	1.40	3.15	0.16	-0.07	10.93
MIROC-ESM	12.65	19.12	0.64	-5.83	1.47	7.23	10.72	0.47	-0.48	4.46
MIROC-ESM-CHEM	13.38	19.80	0.53	-2.15	2.07	8.08	11.59	0.49	-0.21	3.61
MPI-ESM-LR	7.70	15.08	0.73	-2.95	4.50	3.41	6.35	0.38	-0.19	8.64
MPI-ESM-MR	7.90	15.62	0.84	4.41	4.28	3.54	7.06	0.48	0.24	8.39
MPI-ESM-P	7.91	15.69	0.75	-0.25	4.34	3.48	6.48	0.45	0.05	8.56
MRI-CGCM3	13.43	15.99	0.66	1.52	1.67	10.72	13.05	0.63	0.22	2.04

Data sources or CMIP5 models	(a)	(b)	(c)	(d)	(e)	(f)	(g)	(h)	(i)	(j)
MRI-ESM1	13.24	16.32	0.75	-0.62	1.53	10.14	13.00	0.58	-0.03	2.25
NorESM1-M	13.08	14.19	0.57	-0.71	1.24	13.88	12.41	1.17	-0.07	3.66
NorESM1-ME	16.98	14.19	0.60	-3.77	5.24	17.57	16.82	1.40	-0.74	6.59

399

400 Table 2. Arctic sea ice metrics in CMIP5 models, satellite observations and PIOMAS dataset. Column (a) is mean annual SIE in million km².
401 Column (b) is monthly SIE amplitude in million km². Column (c) is standard deviation of detrended monthly SIE anomaly in million km².
402 Column (d) is linear trend in monthly SIE in 10⁵ km² decade⁻¹. Column (e) is monthly SIE room mean square error in million km². Column (f) is
403 mean annual SIV in 10³ km³. Column (g) is monthly SIV amplitude in 10³ km³. Column (h) is standard deviation of detrended monthly SIV
404 anomaly in 10³ km³. Column (i) is linear trend in monthly SIV in 10³ km³ decade⁻¹. Column (j) is monthly SIV room mean square error in 10³
405 km³.

Data sources or CMIP5 models	(a)	(b)	(c)	(d)	(e)	(f)	(g)	(h)	(i)	(j)
Observations or PIOMAS	12.02	8.80	0.29	-4.35	----	21.85	16.17	1.02	-2.14	----
Multi-model ensemble mean (MME)	12.81	10.40	0.13	-3.71	1.07	18.45	17.50	0.35	-1.45	3.57
ACCESS1.0	12.13	10.33	0.41	-5.51	0.94	15.41	18.74	1.05	-1.58	6.60
ACCESS1.3	11.79	9.47	0.43	-0.78	0.73	18.81	17.02	1.02	-1.05	3.23
BCC-CSM1.1	14.86	15.39	0.69	-8.79	3.70	14.29	22.70	1.00	-2.01	8.02

Data sources or CMIP5 models	(a)	(b)	(c)	(d)	(e)	(f)	(g)	(h)	(i)	(j)
BCC-CSM1-1-M	13.19	15.96	0.65	-5.19	2.87	11.04	20.69	0.87	-0.74	11.02
BNU-ESM	14.72	12.61	0.50	-4.41	3.19	23.03	19.79	1.23	-4.37	1.83
CanCM4	12.79	14.77	0.52	-4.97	2.49	11.41	15.35	0.97	-0.38	10.47
CanESM2	12.01	13.76	0.49	-6.80	1.91	9.97	14.21	0.63	-1.18	11.92
CCSM4	12.33	8.56	0.44	-1.34	0.42	20.27	16.16	1.51	-1.54	1.82
CESM1-BGC	12.10	7.96	0.41	-2.85	0.35	20.30	15.52	1.51	-2.63	1.86
CESM1-CAM5	12.33	8.35	0.38	-1.87	0.52	22.73	16.01	1.96	-1.22	1.35
CESM1-CAM5-1-FV2	12.52	8.68	0.42	-5.07	0.64	23.17	16.01	1.87	-3.63	1.49
CESM1-FASTCHEM	12.02	8.86	0.39	-3.70	0.25	18.27	15.86	1.37	-1.98	3.69
CESM1-WACCM	13.44	8.10	0.36	-2.88	1.51	27.32	9.47	2.07	0.09	6.27
CMCC-CESM	13.97	9.33	0.36	-2.63	2.12	28.75	11.93	1.38	-1.44	7.11
CMCC-CM	13.99	7.35	0.30	-5.09	2.06	33.01	9.87	1.73	-2.40	11.52
CMCC-CMS	12.64	7.92	0.34	-2.87	0.82	28.29	9.73	1.29	-1.18	6.89
CNRM-CM5	12.41	11.41	0.46	-7.58	1.11	14.44	20.22	0.99	-1.76	7.60
CNRM-CM5-2	14.20	10.65	0.45	-2.32	2.40	20.11	21.83	1.29	-0.96	2.76
CSIRO-Mk3.6	16.13	7.57	0.30	-5.33	4.20	25.94	12.16	0.81	-2.32	4.30
EC-EARTH	12.45	8.04	0.35	-3.84	0.57	24.01	12.44	1.90	-0.59	2.86
FGOALS-g2	11.68	3.35	0.13	-1.44	1.86	-----	----	----	----	----
FIO-ESM	12.46	10.27	0.40	-2.23	1.00	18.94	18.96	1.86	-1.69	3.15

Data sources or CMIP5 models	(a)	(b)	(c)	(d)	(e)	(f)	(g)	(h)	(i)	(j)
GFDL-CM2p1	12.58	12.85	0.54	-3.76	1.68	11.11	18.13	0.87	-1.01	10.80
GFDL-CM3	12.22	8.71	0.33	-2.89	0.41	15.25	15.47	1.31	-1.18	6.61
GFDL-ESM2G	15.72	13.72	0.48	-7.05	4.24	16.91	19.33	1.24	-1.77	5.17
GFDL-ESM2M	12.46	11.06	0.53	-0.31	0.98	12.13	16.11	1.02	-0.56	9.75
GISS-E2-H	12.96	14.87	0.54	-5.07	2.47	13.61	25.67	0.76	-0.91	9.10
GISS-E2-H-CC	13.94	14.24	0.60	-5.91	2.80	14.94	27.49	0.80	-1.29	8.23
GISS-E2-R	13.65	15.17	0.49	-6.31	2.89	15.50	29.32	0.75	-1.28	8.17
GISS-E2-R-CC	15.13	16.73	0.48	-5.65	4.28	17.16	31.86	0.76	-1.08	7.64
HadCM3	13.94	13.59	0.56	-4.74	2.78	21.07	26.96	0.87	-2.25	4.46
HadGEM2-AO	11.38	10.75	0.40	-3.81	1.15	16.58	20.16	0.84	-0.98	5.53
HadGEM2-CC	13.20	10.68	0.45	-3.10	1.45	21.56	21.55	0.96	-2.47	2.22
HadGEM2-ES	12.34	11.21	0.43	-6.03	1.14	18.85	21.13	1.00	-1.69	3.64
INMCM4	12.92	12.02	0.42	-0.21	1.61	15.20	22.08	0.96	-0.21	7.07
IPSL-CM5A-LR	12.72	10.07	0.44	-3.03	1.14	21.87	16.41	1.48	-0.96	1.66
IPSL-CM5A-MR	11.06	9.55	0.35	-2.85	1.25	14.83	16.32	0.92	-1.69	7.17
IPSL-CM5B-LR	14.06	8.28	0.40	-0.77	2.08	27.28	13.11	2.91	-1.37	6.25
MIROC4h	10.66	9.65	0.40	-3.11	1.47	10.86	16.48	0.82	-1.00	11.02
MIROC5	12.12	6.63	0.29	-6.78	0.65	25.31	14.88	1.09	-3.68	3.81
MIROC-ESM	10.40	8.05	0.34	-1.91	1.69	11.09	14.36	0.62	-1.04	10.79

Data sources or CMIP5 models	(a)	(b)	(c)	(d)	(e)	(f)	(g)	(h)	(i)	(j)
MIROC-ESM-CHEM	10.83	7.89	0.46	-4.24	1.30	12.59	14.73	1.39	-1.69	9.29
MPI-ESM-LR	11.10	7.95	0.40	-2.48	1.01	15.07	16.87	0.85	-1.23	6.85
MPI-ESM-MR	11.07	8.00	0.40	-4.94	1.02	15.20	17.30	0.90	-1.75	6.74
MPI-ESM-P	10.94	8.27	0.34	-1.83	1.13	13.45	17.05	1.13	-0.80	8.46
MRI-CGCM3	15.01	15.27	0.47	-1.44	3.97	15.70	19.40	1.48	-0.55	6.33
MRI-ESM1	14.65	14.67	0.61	-4.07	3.52	15.21	18.89	1.74	-1.56	6.76
NorESM1-M	12.01	5.96	0.25	-1.98	0.90	23.77	11.23	1.57	-0.68	3.11
NorESM1-ME	12.47	5.99	0.31	-0.21	0.97	23.97	9.71	2.14	-0.46	3.69